Theoretical simulations of the effects of the indium content, thickness, and defect density of the *i*-layer on the performance of *p-i-n* InGaN single homojunction solar cells

Shih-Wei Feng,[1,a)] Chih-Ming Lai,[2] Chien-Hsun Chen,[3] Wen-Ching Sun,[4] and Li-Wei Tu[5]
[1]*Department of Applied Physics, National University of Kaohsiung, Taiwan, Republic of China*
[2]*Department of Electronic Engineering, Ming Chuan University, Taoyuan, Taiwan, Republic of China*
[3]*Green Energy and Environment Research Laboratories, Industrial Technology Research Institute, Taiwan, Republic of China*
[4]*Material and Chemical Research Laboratories, Industrial Technology Research Institute, Taiwan, Republic of China*
[5]*Department of Physics and Center for Nanoscience and Nanotechnology, National Sun Yat-Sen University, Taiwan, Republic of China*

(Received 29 June 2010; accepted 10 August 2010; published online 11 November 2010)

In this study, we conducted numerical simulations with the consideration of microelectronic and photonic structures to determine the feasibility of and to design the device structure for the optimized performance of InGaN *p-i-n* single homojunction solar cells. Operation mechanisms of InGaN *p-i-n* single homojunction solar cells were explored through the calculation of the characteristic parameters such as the absorption, collection efficiency (χ), open circuit voltage (V_{oc}), short circuit current density (J_{sc}), and fill factor (FF). Simulation results show that the characteristic parameters of InGaN solar cells strongly depend on the indium content, thickness, and defect density of the *i*-layer. As the indium content in the cell increases, J_{sc} and absorption increase while χ, V_{oc}, and FF decrease. The combined effects of the absorption, χ, V_{oc}, J_{sc}, and FF lead to a higher conversion efficiency in the high-indium-content solar cell. A high-quality $In_{0.75}Ga_{0.25}N$ solar cell with a 4 μm *i*-layer thickness can exhibit as high a conversion efficiency as $\sim$23%. In addition, the similar trend of conversion efficiency to that of J_{sc} shows that J_{sc} is a dominant factor to determine the performance of *p-i-n* InGaN solar cells. Furthermore, compared with the previous simulation results without the consideration of defect density, the lower calculated conversion efficiency verifies that the sample quality has a great effect on the performance of a solar cell and a high-quality InGaN alloy is necessary for the device fabrication. Simulation results help us to better understand the electro-optical characteristics of InGaN solar cells and can be utilized for efficiency enhancement through optimization of the device structure. © *2010 American Institute of Physics*. [doi:10.1063/1.3484040]

I. INTRODUCTION

InGaN wide band gap semiconductors have become the key technological material for light emitting diodes and laser diodes.[1–3] The application of InGaN semiconductors for solar cells is still a promising prospect. The band gap of InGaN alloys, ranging from 0.7 to 3.4 eV, can fit the full solar spectrum.[1] This offers a great advantage in designing and fabricating high-efficiency tandem solar cells. InGaN/GaN, InGaN/Si, and InGaN/Ge heterojunction solar cells have been demonstrated to exhibit a high-performance photovoltaic effects, such as high fill factor (FF), high carrier mobility, high saturation velocity, high temperature resistance, and superior radioresistance.[4–6] In addition, the III-nitride semiconductors exhibit high absorption coefficient of approximately 10^5 cm^{-1} near the band edge such that most of the incident light would be absorbed in only a few hundred nanometers.[7–9] This is in contrast to the traditional Si-based solar cells with several microns in thickness.

Currently, the III-nitride system suffers some challenges to the device application and the reported InGaN-based solar cells show a low conversion efficiency of less than 2%.[10–13] The III-nitride semiconductors are less mature than other III–V semiconductors and do not show as high an efficiency as other III–V compound semiconductors. Because of the lack of defect-free native substrates, the III-nitride epilayers grown on sapphire substrates contain high densities of threading dislocation, stacking fault, and V-shaped defect, leading to the degradation of device performance.[14] Also, due to the large lattice mismatch between InN and GaN, their low miscibility leads to indium aggregation and phase separation, making it difficult to grow good quality InGaN with a high In content.[14] The phenomena show that a high-quality InGaN is essential for the application of high-performance solar cells.

Besides device fabrication, numerical simulations of InGaN single-junction and multijunction solar cells were conducted. The performance of $In_{0.65}Ga_{0.35}N$ single-junction solar cells with different doping densities and thicknesses of each layer have been theoretically simulated.[10] The efficiencies of $In_xGa_{1-x}N$ multijunction tandem solar cells with vari-

a)Electronic mail:swfeng@nuk.edu.tw.

ous thickness and indium composition were theoretically calculated to be 27.49% and 40.35% for the double- and six-junction solar cells, respectively.[11] Also, the efficiency of InGaN seven-junction tandem solar cells was predicted to be as high as 46.01%.[12] Furthermore, because the conduction band of $In_{0.46}Ga_{0.54}N$ has the same energy as the valence band of Si, a n-$In_{0.46}Ga_{0.54}N/p$-Si interface should form a low resistance Ohmic junction without heavy doping of the interface between the two materials.[13] The band gap combination of $In_{0.46}Ga_{0.54}N(1.8\ \text{eV})/\text{Si}(1.1\ \text{eV})$ would give the maximum energy conversion efficiency for double-junction solar cells. High quality double-junction InGaN/Si solar cells under optimized conditions of InGaN band gap and Si junction thickness were estimated to produce an energy conversion efficiency around 30%–32%.[13] Although the efficiencies of InGaN/InGaN and InGaN/Si heterojunction tandem cells were theoretically determined, the characteristics of the basic component, InGaN single-junction cell, of the heterojunction and tandem solar cells were not well understood. In particular, the influences of structure design and defect density on the performance of the *p*-*i*-*n* InGaN single-junction cell should be studied further.

In this study, we conduct numerical simulations to design the device structure for the optimized performance of InGaN *p*-*i*-*n* single homojunction solar cells. Simulation results show that the collection efficiency, short circuit current density, open circuit voltage, and conversion efficiency strongly depend on the indium content, thickness, and defect density of the *i*-layer. It was verifies that the sample quality has a great effect on the performance of solar cells and a high-quality InGaN alloy is necessary for the device fabrication. Besides a high-quality InGaN alloy, the series resistance and leakage current should be minimized to achieve a high-performance solar cell. Simulation results help us better understand the operation mechanisms, and can be used to optimize the performance, of InGaN solar cells.

This paper is organized as follows: in Sec. II, theoretical modeling is described. In Sec. III, simulation results of InGaN *p*-*i*-*n* InGaN single-junction cells are discussed. Finally, conclusions are drawn in Sec. IV.

II. THEORETICAL MODELING

p-*i*-*n* solar cells have some advantages compared to *p*-*n* diodes. Because *p*-*n* diode is limited by the reverse current breakdown, a thin intrinsic layer (*i*-layer) or absorption layer is preferentially used to enhance the built-in field and completely deplete the charge carriers. This leads to a large prompt current and a high quantum efficiency. Figure 1 shows the structure of an InGaN *p*-*i*-*n* single homojunction solar cell for simulation. The thickness of *p*-layer is assumed to be 50 nm. The *i*-layer is the most important layer, because photons absorbed in the *i*-layer generate electron-hole pairs. The charge carriers are separated by the internal field provided by the *p*- and *n*-layers and collected at the electrodes. Therefore, the thickness and defect density in the *i*-layer will greatly affect the performance of the solar cells. The characteristic parameters of the solar cells were simulated as a function of the indium content, thickness, and defect density of the *i*-layer. Simulations were performed using in-house code written for MATLAB (MathWorks Inc.).

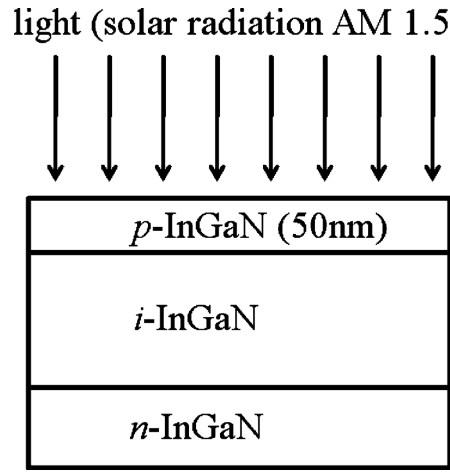

FIG. 1. The *p*-*i*-*n* structure of InGaN single homojunction solar cells for theoretical simulation. The solar cell is under AM 1.5 G illumination ($100\ \text{mW/cm}^2$).

In the numerical simulations, we modified the theoretical model proposed to design the structures of *p*-*i*-*n* amorphous silicon solar cells.[15,16] The number of photons as a function of energy, $P_{i\text{-layer}}(E)$, absorbed in the *i*-layer can be written as:

$$P_{i\text{-layer}}(E) = \frac{A(E)F(E)}{E}, \tag{1}$$

where $F(E)$ is incident flux of solar radiation air mass (AM) 1.5 ($100\ \text{mW/cm}^2$), $E(=h\nu)$ is the energy of photons, and $A(E)$ is absorbance of the *i*-layer. The absorbance of the *i*-layer, $A(E)$, can be defined as

$$A(E) = \frac{I(E,z=50\ \text{nm}) - I(E,z=50\ \text{nm}+i\ \text{thickness})}{I_0(E)}. \tag{2}$$

When the light penetrates into the solar cell, the light intensity decays exponentially. With the consideration of the absorption of the *p*-layer, the intensity will be attenuated by a factor $e^{-\alpha z}$,[1] where $z(=50\ \text{nm})$ is the thickness of the *p*-layer and α is the absorption coefficient of InGaN in the *p*-layer. Before reaching the *i*-layer, the intensity becomes

$$I(E,z) = I_0(E)e^{-\alpha(E)z}, \tag{3}$$

where I_0 is the incident intensity of solar radiation AM 1.5 ($100\ \text{mW/cm}^2$). In an idealized semiconductor, the absorption coefficient $\alpha(E)$ as a function of energy can be expressed as[17]

$$\alpha(E) = \alpha_0\sqrt{\frac{E - E_g(x)}{E_g(x)}}, \tag{4}$$

where $E_g(x)$ is the band gap of $In_xGa_{1-x}N$ and α_0 is about $2\times10^5\ \text{cm}^{-1}$ for GaN.[1] The α_0 of the InGaN is assumed to be the same as that of GaN. The band gap energy $E_g(x)$ of $In_xGa_{1-x}N$ ternary alloy can be expressed as[17]

$$E_g(x) = 0.7x + 3.4(1-x) - 1.43x(1-x) \ \ (\text{eV}). \tag{5}$$

Assuming that each absorbed photon creates a pair of charge carriers (electron and hole) in the i-layer, the optically limited current in the i-layer can be obtained as

$$J_{i\text{-layer}} = q\int P_{i\text{-layer}}(E)dE = q\int \frac{A(E)F(E)}{E}dE, \tag{6}$$

where q is the electronic charge $(1.6\times 10^{-19}C)$.

The short circuit current density, J_{sc}, in the cell can be obtained as the product of the number of photogenerated charge carriers and collection efficiency

$$J_{sc} = q\chi\int \frac{A(E)F(E)}{E}dE, \tag{7}$$

where χ is the collection efficiency. The collection efficiency of a p-i-n solar cell is defined as the ratio of the number of charge carriers contributing of the photovoltaic current to the total number of photogenerated charge carriers. The collection efficiency is an important parameter in determining the performance of a solar cell. Depending on the thickness and defect density of the i-layer, χ is between 0 and 1. Before the computation of J_{sc}, the collection efficiency should be obtained. χ in the i-layer can be written as[15,16]

$$\chi = \frac{\int_0^L (G-R)dx}{\int_0^L G dx} \cong \frac{G_0 L - \int_0^L R(x)dx}{G_0 L}, \tag{8}$$

where G and R are the generation rate and recombination rate of charge carriers, respectively, and L is the thickness of the i-layer. In general, the generation rate, G, depends on the absorption profile of the i-layer and is not a constant. Here, $G=G_0$ is assumed to be a constant through the i-layer. The recombination function, $R(x)$, can be calculated as

$$R(x) = \frac{n(x)}{\tau_n} + \frac{p(x)}{\tau_p}, \tag{9}$$

where τ_n and τ_p are the electron and hole capture times by defects, respectively, and $n(x)$ and $p(x)$ are electron and hole concentrations, respectively. $n(x)$ and $p(x)$ must be obtained by solving the steady state continuity and transport equations given by

$$0 = G_0 - R(x) + \frac{1}{q}\frac{d}{dx}J_n(x), \tag{10a}$$

$$0 = G_0 - R(x) - \frac{1}{q}\frac{d}{dx}J_p(x), \tag{10b}$$

$$J_n(x) = q\mu_n n(x)E_0, \tag{11a}$$

$$J_p(x) = q\mu_p p(x)E_0, \tag{11b}$$

where q is the electron charge, $J_n(x)$ and $J_p(x)$ are the electron and hole current densities, respectively, μ_n and μ_p are the electron and hole mobilities, respectively. By solving Eqs. (10) and (11), we can get $n(x)$ and $p(x)$ (Refs. 15 and 16)

$$n(x) = \frac{G_0 l_p \tau_n}{l_p - l_n e^{-bL}}(1-e^{-bx}), \tag{12a}$$

$$p(x) = \frac{G_0 l_n \tau_p}{l_p - l_n e^{-bL}}(e^{-bx} - e^{-bL}), \tag{12b}$$

where $b=l_n-l_p/-l_nl_p=-(2/L_c)$.

Then

$$\int_0^L R(x)dx = \int_0^L \left(\frac{n(x)}{\tau_n} + \frac{p(x)}{\tau_p}\right)dx = \frac{C_3 l_p}{b}[Lb - (1-e^{-bL})] + \frac{C_3 l_n}{b}[1 - e^{-bL}(1+bL)] = \frac{G_0 l_n l_p (e^{-bL}-1)}{l_p - l_n e^{-bL}} + LG_0. \tag{13}$$

We get the expression for χ as[15,16]

$$\chi = \frac{G_0 L - \int_0^L R(x)dx}{G_0 L} = \frac{1}{L}\frac{l_n l_p}{l_n \exp\left(\frac{L}{L_c}\right) - l_p \exp\left(-\frac{L}{L_c}\right)}\left[\exp\left(\frac{L}{L_c}\right) - \exp\left(-\frac{L}{L_c}\right)\right], \tag{14}$$

where $L_c=2(l_nl_p/l_n-l_p)$, $l_n=\mu_n\tau_nE_0$, and $l_p=\mu_p\tau_pE_0$ are drift lengths of free electrons and holes, respectively, E_0 is the internal electric field provided by p- and n-layers, and $\mu_n(=1000\ \text{cm}^2/\text{V s})$ and $\mu_p(=170\ \text{cm}^2/\text{V s})$ are electron and hole mobilities, respectively.[10]

In semiconductors, the recombination process of photogenerated electrons and holes can be either photon emission in a radiative event or nonradiative recombination via defects and the Auger process.[18] High-indium-content InGaN alloys often lead to a low crystalline quality because of indium aggregation and/or phase separation.[14] High densities of threading dislocations, stacking faults, and V-shaped defects in the III-nitride epilayers lead to the degradation of device performance.[14] Hence, the carrier lifetime at room temperature is assumed to be dominated by the nonradiative recombination. According to Shockley–Read–Hall theory, the nonradiative lifetime through defect-assisted recombination in deep levels can be expressed as[18]

$$\tau_n = \frac{1}{\sigma_n \times v_{\text{thermal}} \times N_d}, \tag{15a}$$

$$\tau_p = \frac{1}{\sigma_p \times v_{\text{thermal}} \times N_d}, \tag{15b}$$

where σ_n(=2.7×10^{-21} cm^2) and σ_p(=2.7×10^{-14} cm^2) are the electron and hole capture cross sections, respectively.[19] N_d is the defect density (cm^{-3}) and v_{thermal}(=10^7 cm/s) is the thermal velocity of the carriers at the room temperature. Hence, drift lengths of free electrons and holes can be expressed as

$$l_n = \mu_n \tau E_0 = \mu_n \frac{1}{\sigma_n \times v_{\text{thermal}} \times N_d} \frac{V_{bi}}{L} = \frac{\mu_n \times V_{bi}}{\sigma_n \times v_{\text{thermal}} \times N_d \times L}, \tag{16a}$$

$$l_p = \mu_p \tau E_0 = \mu_p \frac{1}{\sigma_p \times v_{\text{thermal}} \times N_d} \frac{V_{bi}}{L} = \frac{\mu_p \times V_{bi}}{\sigma_p \times v_{\text{thermal}} \times N_d \times L}, \tag{16b}$$

where V_{bi} is the built-in voltage. For $In_xGa_{1-x}N$ light emitting diodes, the built-in voltage can be approximated by the band gap energy $E_g(x)$ divided by the elementary charge q (Ref. 1)

$$V_{bi} \cong E_g(x)/q = [0.7x + 3.4(1-x) - 1.43x(1-x)]/q(V). \tag{17}$$

The indium compositions are set at 0.12, 0.46, and 0.75.

In addition, the open circuit voltage, V_{oc}, can be expressed as

$$V_{oc} = \frac{n_{\text{ideal}} kT}{q} \ln\left(\frac{J_{sc}}{J_o} + 1\right). \tag{18}$$

where n_{ideal} is the ideality factor. Typically, $n_{\text{ideal}} \cong 1.1-1.5$ for III–V real diodes.[1] We assume n_{ideal} to be 1.2. q is the elementary charge. J_0 is the saturation current. The expressions of J_0 for a *p-n* solar cell and a *p-i-n* one are different.[20] For a *p-i-n* thin film solar cell, the Sah–Noyce–Shockley approximation is valid and J_0 can be expressed as

$$J_0 = \frac{q n_i L}{\sqrt{\tau_n \tau_p}}, \tag{19}$$

where n_i is the intrinsic carrier concentration.[20] The intrinsic carrier concentration, n_i, can be expressed as:[11]

$$n_i^2 = 2.31 \times 10^{31} \left(\frac{m_{nd} m_{pd}}{m_0^2}\right)^{3/2} \times T^3 \times \exp\left[-\frac{E_g(x)}{kT}\right]. \tag{20}$$

For GaN, m_{nd}=$0.2m_0$ and m_{pd}=$0.8m_0$; m_0 is the electron rest mass. We take the parameters of GaN instead of InGaN to calculate J_0.

Furthermore, the maximum power point is a point on the current-voltage (*I-V*) curve that gives maximum power output $P_{\max}$.

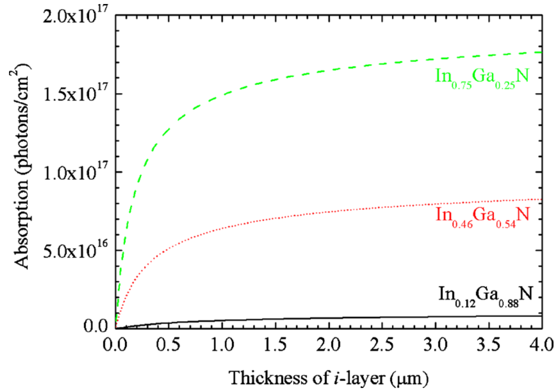

FIG. 2. (Color online) Absorption as a function of *i*-layer thickness for $In_{0.12}Ga_{0.88}N$, $In_{0.46}Ga_{0.54}N$, and $In_{0.75}Ga_{0.25}N$ single homojunction solar cells.

$$P_{\max} = J_m V_m, \tag{21}$$

where J_m and V_m correspond to the values of I and V at $P_{\max}$, respectively. The *FF* of a solar cell is calculated as

$$FF = \frac{P_{\max}}{J_{sc} V_{oc}} = \frac{J_m V_m}{J_{sc} V_{oc}}. \tag{22}$$

The conversion efficiency, η, of a solar cell can be expressed as

$$\eta = \frac{P_{\max}}{P_{in}} = \frac{FF \times J_{sc} \times V_{oc}}{P_{in}}, \tag{23}$$

where P_{in} is the optical input power of solar radiation AM 1.5 G illumination (100 mW/cm^2) on the surface of solar cells.

III. SIMULATION RESULTS AND DISCUSSIONS

Figure 2 shows the absorption of $In_{0.12}Ga_{0.88}N$, $In_{0.46}Ga_{0.54}N$, and $In_{0.75}Ga_{0.25}N$ single homojunction solar cells under AM 1.5 G illumination (100 mW/cm^2). As the thickness of the *i*-layer increases, the *i*-layer can absorb more photons. Photons absorbed in the *i*-layer generate electron-hole pairs which are separated by the built-in field (E_0). The photogenerated current depends on the absorption photons and collection efficiency in the *i*-layer. In addition, as the indium content in the cell increases, the absorption of photons also increases. With a small band gap in the high-indium solar cell, more photons with energy larger than the band gap can be absorbed. In particular, the stronger intensity of the solar radiation spectrum in the visible range enhances the absorption. The deeper penetration of the photons in the infrared range also enhances the photon absorption.

Figure 3 shows the collection efficiency as a function of *i*-layer thickness for $In_{0.12}Ga_{0.88}N$, $In_{0.46}Ga_{0.54}N$, and $In_{0.75}Ga_{0.25}N$ single homojunction solar cells with various defect densities. Simulation results show that the collection efficiency strongly depends on the indium content, thickness, and defect density of the *i*-layer. This verifies that a high-quality InGaN alloy is required for the application of high-efficiency solar cells. In the low-defect-density range (10^8-10^{14} cm^{-3}), the collection efficiency is nearly unity and independent of the indium content, thickness, and defect

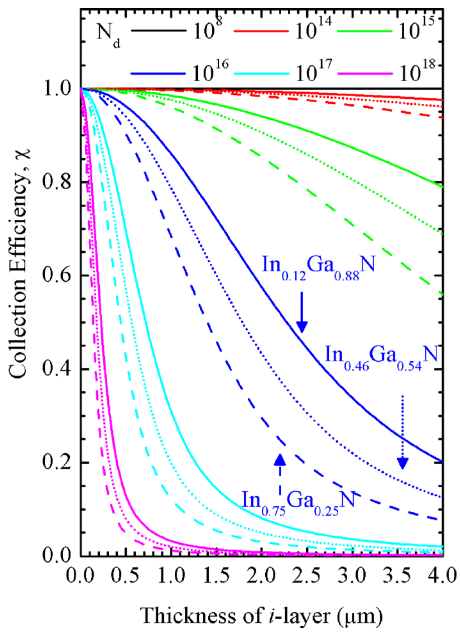

FIG. 3. (Color online) Collection efficiency as a function of *i*-layer thickness for $In_{0.12}Ga_{0.88}N$, $In_{0.46}Ga_{0.54}N$, and $In_{0.75}Ga_{0.25}N$ single homojunction solar cells with various defect densities. $In_{0.12}Ga_{0.88}N$, $In_{0.46}Ga_{0.54}N$, and $In_{0.75}Ga_{0.25}N$ are represented by solid (—), dotted (···), and dashed (- - -) lines, respectively.

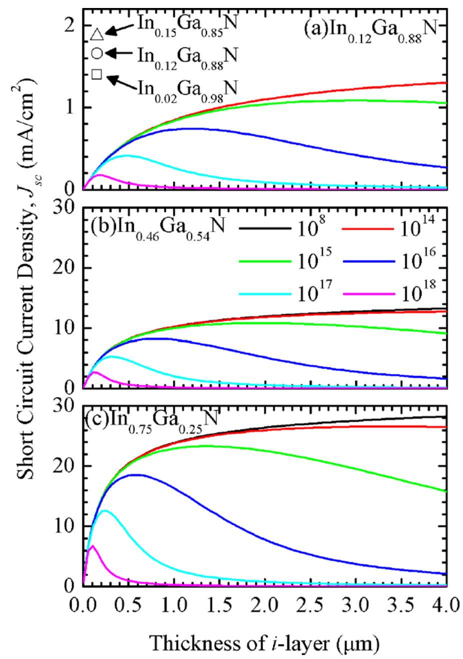

FIG. 4. (Color online) Short circuit current density, J_{sc}, as a function of *i*-layer thickness for (a) $In_{0.12}Ga_{0.88}N$, (b) $In_{0.46}Ga_{0.54}N$, and (c) $In_{0.75}Ga_{0.25}N$ single homojunction solar cells with various defect densities. The reported J_{sc} of $In_{0.02}Ga_{0.98}N$ (□), $In_{0.12}Ga_{0.88}N$ (○), and $In_{0.15}Ga_{0.85}N$ (△) *p-i-n* homojunction solar cells with *i*-thickness 150 nm are plotted in Fig. 4(a) for comparison (Ref. 4).

density of the *i*-layer. This implies that good-quality InGaN alloy can achieve high-collection efficiency and is suitable for the fabrication of high-efficiency InGaN solar cells. In general, a larger *i*-layer thickness of a solar cell results in a smaller built-in field (E_0) and, hence, smaller drift lengths of free electrons and holes. Although smaller drift lengths make it difficult for the charge carriers to reach the electrodes, good sample quality prevents the charge carriers from being captured by the defects. Hence, a high collection efficiency and a smaller defect capture rate were observed in a good-quality InGaN solar cell.

On the other hand, in the high defect density range (10^{15}–10^{18} cm^{-3}), as the *i*-layer thickness of the solar cell increases, the collection efficiency starts to decrease. In particular, when the defect density equals to 10^{18} (cm^{-3}), the collection efficiency drops dramatically. According to Eq. (15), a higher defect density results in a shorter lifetime and, hence, a lower diffusion length. Carriers generated in the *i*-layer cannot successfully drift to the contacts of the device before recombination and do not contribute to the photocurrent. Hence, the separated charge carriers were easily captured by the high density defects and the solar cell would exhibit a low-collection efficiency. Furthermore, for the cell corresponding to the same defect density and thickness of the *i*-layer, the collection efficiency becomes lower in the high-indium-content cell. In general, a small band gap and a small built-in voltage lead to the electrons and holes showing shorter drift lengths. Carriers generated in the *i*-layer drift only slightly toward the contacts of the device before recombination and were more easily captured by the high density defects. Hence, if this solar cell were built, it would exhibit a low collection efficiency.

Figures 4(a)–4(c) show the short circuit current densities, J_{sc}, of $In_{0.12}Ga_{0.88}N$, $In_{0.46}Ga_{0.54}N$, and $In_{0.75}Ga_{0.25}N$ single homojunction solar cells, respectively. J_{sc} shows a strong dependence on the indium content, thickness, and defect density of the *i*-layer. According to Eq. (7), J_{sc} can be expressed as the product of the collection efficiency and the generated charge carriers. As shown in Fig. 2, a thicker *i*-layer would absorb more photons and generate more electron-hole pairs. In the low-defect-density range (10^8–10^{14} cm^{-3}), a high collection efficiency would increase J_{sc} in the thicker solar cells. In the high-defect-density range (10^{15}–10^{18} cm^{-3}), although a thicker *i*-layer would absorb more photons and generate more electron-hole pairs, the inefficient collection efficiency results in a decreasing of J_{sc}. In addition, the J_{sc} of the $In_{0.75}Ga_{0.25}N$ solar cell corresponding to the same defect density and thickness of the *i*-layer is about one order of magnitude larger than that of the $In_{0.12}Ga_{0.88}N$ solar cell. This shows that a larger absorption increase J_{sc} and the effect of absorption in the cell are more dominant than the effect of the collection efficiency. Furthermore, the reported J_{sc} of $In_{0.02}Ga_{0.98}N$ (□), $In_{0.12}Ga_{0.88}N$ (○), and $In_{0.15}Ga_{0.85}N$ (△) *p-i-n* homojunction solar cells with *i*-layer thickness 150 nm are plotted in Fig. 4(a) for comparison.[4] The reported J_{sc} becomes larger in the high-indium-content solar cell. The trend is consistent with our simulation results. Also, for $In_{0.12}Ga_{0.88}N$ *p-i-n* homojunction solar cell, simulation result of J_{sc} is smaller than that obtained by device measurement. This could be due to different illumination sources and power densities. In general, the J_{sc} of solar cells strongly depends on the power density of the illumination source.[20] Our illumination source for the-

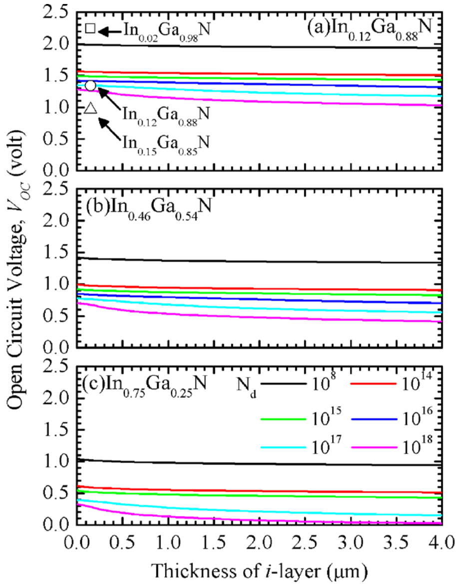

FIG. 5. (Color online) Open circuit voltage, V_{oc}, as a function of *i*-layer thickness for (a) $In_{0.12}Ga_{0.88}N$, (b) $In_{0.46}Ga_{0.54}N$, and (c) $In_{0.75}Ga_{0.25}N$ single homojunction solar cells with various defect densities. The reported V_{oc} of $In_{0.02}Ga_{0.98}N$ (□), $In_{0.12}Ga_{0.88}N$ (○), and $In_{0.15}Ga_{0.85}N$ (△) *p-i-n* homojunction solar cells with *i*-thickness 150 nm are plotted in Fig. 5(a) for comparison (Ref. 4).

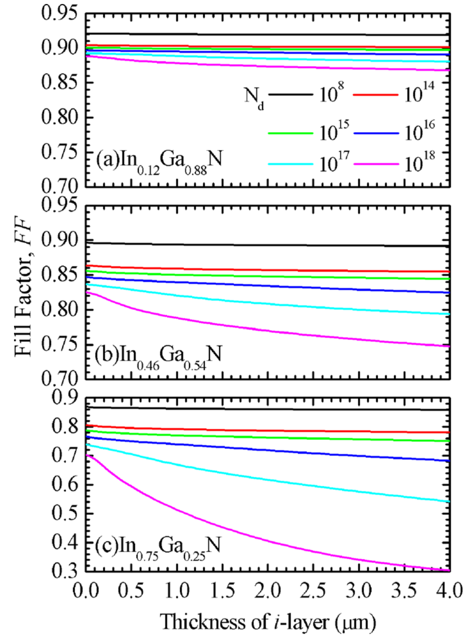

FIG. 6. (Color online) *FF* as a function of *i*-layer thickness for (a) $In_{0.12}Ga_{0.88}N$, (b) $In_{0.46}Ga_{0.54}N$, and (c) $In_{0.75}Ga_{0.25}N$ single homojunction solar cells with various defect densities.

oretical simulation is solar radiation AM 1.5 (100 mW/cm^2), while that for the device measurement is a xenon lamp (unknown power density).[20]

Figure 5 shows the open circuit voltage, V_{oc}, of $In_{0.12}Ga_{0.88}N$, $In_{0.46}Ga_{0.54}N$, and $In_{0.75}Ga_{0.25}N$ single homojunction solar cells. Simulation results show that V_{oc} depends on the defect density but only very slightly on the *i*-layer thickness. This result is consistent with the fact that InGaN *p-i-n* homojunction solar cells with higher densities of defects and dislocations exhibit a larger dark current and lower V_{oc}.[4] In addition, due to the natural logarithm between V_{oc} and J_{sc}, V_{oc} should show a similar trend, but with less variation, compared to J_{sc}, for the cells with the same indium content. However, V_{oc} starts to decrease slightly in the thicker cell, due to the larger saturation current, J_0, in the thicker cell. In the high-indium-content cell, V_{oc} is smaller. This is also due to the larger saturation current, J_0, in the high-indium-content cell. Furthermore, the reported V_{oc} of $In_{0.02}Ga_{0.98}N$ (□), $In_{0.12}Ga_{0.88}N$ (○), and $In_{0.15}Ga_{0.85}N$ (△) *p-i-n* homojunction solar cells with *i*-layer thickness 150 nm are plotted in Fig. 5(a) for comparison.[4] Our simulation results are consistent with the trend that the reported V_{oc} is smaller in the high-indium-content cell. For the $In_{0.12}Ga_{0.88}N$ *p-i-n* homojunction solar cell, the reported V_{oc} is in the range of our simulation result, but the reported J_{sc} is slightly different from the simulation result. The trend is a typical characteristic of solar cells.[20] In general, J_{sc} of solar cells strongly depends on the power density of the illumination source, while the V_{oc} is less sensitive to that.

Figure 6 shows the *FF* of $In_{0.12}Ga_{0.88}N$, $In_{0.46}Ga_{0.54}N$, and $In_{0.75}Ga_{0.25}N$ single homojunction solar cells. For the $In_{0.12}Ga_{0.88}N$ solar cell, it was found that the *FF* can be as high as 0.92 and does not show large variations with varying defect density and *i*-layer thickness. In general, the III–V solar cells exhibit a high *FF* of 0.80–0.86.[21] Currently, the reported *FF* of low-indium InGaN/GaN multiple quantum well solar cells is about 0.72,[22] while that of low-indium InGaN *p-i-n* homojunction solar cells is only 0.64–0.69.[4] For actual fabricated solar cells, the contact between the semiconductor alloy and the metal results in a series resistance. The generation-recombination current, surface recombination, and edge isolation inside the solar cell lead to a current leakage and hence a shunt resistance. Without consideration of the effects of the current leakage and shunt resistance, the simulation results of *FF* can be higher than those of the actual fabricated solar cells. Hence, besides a high-quality InGaN alloy, the series resistance and leakage current should be minimized to achieve a high-performance solar cell. In addition, for the $In_{0.75}Ga_{0.25}N$ solar cell, the defect density and *i*-layer thickness have great effect on the variations in the *FF*. This is due to the fact that J_{sc} and V_{oc} show larger variations with varying defect density and *i*-layer thickness, as shown in Figs. 4(c) and 5(c), respectively. The smaller *FF* in the high-indium-content solar cell can be attributed to the larger J_{sc}.

Figures 7(a)–7(c) show the conversion efficiency as a function of *i*-layer thickness for $In_{0.12}Ga_{0.88}N$, $In_{0.46}Ga_{0.54}N$, and $In_{0.75}Ga_{0.25}N$ single homojunction solar cells with various defect densities, respectively. Simulation results provide much information for the structure design of *p-i-n* InGaN solar cells. The conversion efficiency represents the combined effects of the absorption, χ, V_{oc}, J_{sc}, and *FF*. As the indium content in the cell increases, J_{sc} and absorption increase while χ, V_{oc}, and *FF* decrease. The combined effects of the absorption, χ, V_{oc}, J_{sc}, and *FF* lead to a higher conversion efficiency in the high-indium-content solar cell. A high-quality $In_{0.75}Ga_{0.25}N$ solar cell with a 4 μm *i*-layer thickness can exhibit as high a conversion efficiency as ~23%. Also, the trend of conversion efficiency is similar to

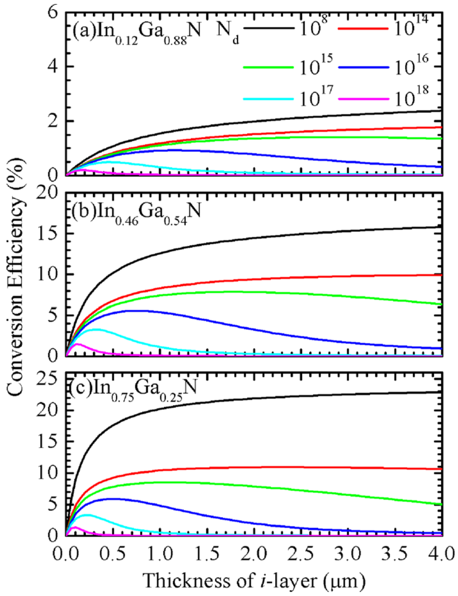

FIG. 7. (Color online) Conversion efficiency as a function of *i*-layer thickness for (a) $In_{0.12}Ga_{0.88}N$, (b) $In_{0.46}Ga_{0.54}N$, and (c) $In_{0.75}Ga_{0.25}N$ single homojunction solar cells with various defect densities.

that of J_{sc}. This shows that J_{sc} is a dominant factor in determining the performance of *p-i-n* InGaN solar cells. In addition, in the low defect density range (10^8–10^{14} cm^{-3}), a larger conversion efficiency can be achieved in the thicker *i*-layer solar cells. This verified that a high-quality InGaN alloy is necessary for the device fabrication. Due to larger values of χ, V_{oc}, J_{sc}, and *FF* in the thicker *i*-layer solar cells, the conversion efficiency increases with increasing *i*-layer thickness. Although a smaller built-in field E_0 may not separate so many charge carriers, a good collection efficiency can compensate for the charge carriers being captured by the defects. By using a high-quality and thick *i*-layer, a high conversion efficiency of *p-i-n* InGaN solar cells can be achieved. Meanwhile, in the high-defect-density range (10^{15}–10^{18} cm^{-3}), the conversion efficiency increases first and then decreases as the *i*-layer thickness increases. In particular, the conversion efficiency dramatically drops when the defect density is larger than 10^{17} (cm^{-3}). Also, compared with the simulation results without the consideration of defect density in the previous study, it was found that the calculated conversion efficiency becomes lower.[10] These both show that the defect density has a great impact on the performance of solar cells. Simulation results of indium content, *i*-layer thickness, and defect density corresponding to maximum conversion efficiency can be used to optimize the performance of InGaN solar cells.

IV. CONCLUSIONS

In summary, numerical simulations to design the optimized structure of InGaN *p-i-n* single homojunction solar cells have been conducted. Simulation results show that the absorption, collection efficiency, short circuit current density, open circuit voltage, and conversion efficiency strongly depend on the indium content, thickness, and defect density of the *i*-layer. The conversion efficiency represents the combined effects of characteristic parameters of InGaN solar cells, which in turn are governed by the device structure and sample quality. In addition, the high-quality $In_{0.75}Ga_{0.25}N$ solar cell with a 4 μm *i*-layer thickness can achieve a high conversion efficiency of ~23%. The trend of conversion efficiency is similar to that of J_{sc}. This shows that J_{sc} is a dominant factor in determining the performance of *p-i-n* InGaN solar cells. Furthermore, compared with previous simulation investigations without the consideration of defect density, it was found that the calculated conversion efficiency becomes a little lower. By appropriate structured design of the devices, the performance of InGaN solar cells can be optimized.

ACKNOWLEDGMENTS

This research was supported by the National Science Council, Taiwan, R.O.C., under Grant Nos. NSC 98-3114-E-110-001 and NSC 99-2515-S-390-001 and by Photovoltaics Technology Center, Industrial Technology Research Institute, Taiwan, R.O.C.

[1] E. Fred Schubert, *Light Emitting Diodes* (Cambridge University Press, New York, 2006).
[2] S. Nakamura and G. Fasol, *The Blue Laser Diode: The Complete Story* (Springer, Berlin, 2000).
[3] S. W. Feng, L. W. Tu, J. I. Chyi, and H. C. Wang, Thin Solid Films **517**, 909 (2008).
[4] X. M. Cai, S. W. Zeng, and B. P. Zhang, Appl. Phys. Lett. **95**, 173504 (2009).
[5] Y. Nanishi, Y. Saito, and T. Yamaguchi, Jpn. J. Appl. Phys., Part 1 **42**, 2549 (2003).
[6] X. Zheng, R. H. Horng, D. S. Wuu, M. T. Chu, W. Y. Liao, M. H. Wu, R. M. Lin, and Y. C. Lu, Appl. Phys. Lett. **93**, 261108 (2008).
[7] C. J. Neufeld, N. G. Toledo, S. C. Cruz, M. Iza, S. P. DenBaars, and U. K. Mishra, Appl. Phys. Lett. **93**, 143502 (2008).
[8] R. Singh, D. Doppalapudi, T. D. Moustakas, and L. T. Romano, Appl. Phys. Lett. **70**, 1089 (1997).
[9] J. F. Muth, J. H. Lee, I. K. Shmagin, R. M. Kolbas, J. Casey, B. P. Keller, U. K. Mishra, and S. P. DenBaars, Appl. Phys. Lett. **71**, 2572 (1997).
[10] X. Zhang, X. L. Wang, H. L. Xiao, C. B. Yang, J. X. Ran, C. M. Wang, Q. F. Hou, and J. M. Li, J. Phys. D: Appl. Phys. **40**, 7335 (2007).
[11] H. Hamzaoui, A. S. Bouazzi, and B. Rezig, Sol. Energy Mater. Sol. Cells **87**, 595 (2005).
[12] Md. R. Islam, A. N. M. E. Kabir, and A. G. Bhuiyan, Istanbul University-Journal of Electrical & Electronics Engineering **6**, 251 (2006).
[13] L. Hsu and W. Walukiewicz, J. Appl. Phys. **104**, 024507 (2008).
[14] Y. S. Lin, K. J. Ma, C. Hsu, S. W. Feng, Y. C. Cheng, C. C. Liao, C. C. Yang, C. C. Chou, C. M. Lee, and J. I. Chyi, Appl. Phys. Lett. **77**, 2988 (2000).
[15] P. Štulik and H. Singh, J. Non-Cryst. Solids **226**, 299 (1998).
[16] J. Hubin, and A. V. Shah, Philos. Mag. B **72**, 589 (1995).
[17] I. Vurgaftman and J. R. Meyer, J. Appl. Phys. **94**, 3675 (2003).
[18] J. Wu, J. Appl. Phys. **106**, 011101 (2009).
[19] M. A. Reshchikov and H. Morkoç, J. Appl. Phys. **97**, 061301 (2005).
[20] Jenny Nelson, *The Physics of Solar Cells* (Imperial College Press, UK, 2003).
[21] M. A. Green, K. Emery, Y. Hishikawa, and W. Warta, Prog. Photovoltaics **17**, 85 (2009).
[22] M. J. Jeng, Y. L. Lee, and L. B. Chang, J. Phys. D: Appl. Phys. **42**, 105101 (2009).